A Frequency-Constrained SC-AC OPF Method with Joint Static and Frequency Security Constraints

Shen-Hao Li
School of Electrical and Information Engineering
Tianjin University
Tianjin, China

Hsiao-Dong Chiang, Fellow, IEEE
School of Electrical and Computer Engineering
Cornell University
Ithaca, NY, USA

***Abstract*—The trend toward low-inertia power systems reveals a critical gap: secure operating points under static N-1 criterion may violate post-contingency frequency response constraints. This paper develops a frequency constrained security-constrained AC optimal power flow (FC-SC-ACOPF) framework considering both static security and frequency security constraints. The proposed framework considers key frequency security metrics, including the frequency nadir and the rate of change of frequency (RoCoF), while retaining the full AC power flow equations for the base case and a set of contingencies to ensure static security. To maintain computational tractability, a dominant contingency identification method is presented to identify dominant contingencies while a trajectory-unified (TJU) methodology is developed for robustly solving the proposed FC-SC-ACOPF formulation. Numerical studies on several test systems including a 500-bus test system were conducted to validate the effectiveness of the proposed framework.**

***Index Terms*—Security-constrained optimal power flow, frequency security, primary frequency response, dominant contingency, trajectory-unified methodology.**

I. INTRODUCTION

Large-scale power systems are increasingly operated with lower synchronous inertia. Consequently, operating points that satisfy static N-1 criterion may fail to maintain post-contingency frequency response within safe limits after a severe contingency. Operating points that are simultaneously N-1 secure and frequency secure are required, yet the two requirements interact in nontrivial ways: enforcing frequency security constraints can significantly change the feasible region of the original problem, resulting in different solutions that may alter compliance with the static N-1 criterion [1].

Frequency security constraints have been integrated into operational scheduling primarily through simplified primary frequency response models in DC-OPF and unit commitment formulations [2-4] or through more detailed dynamic embeddings coupled with AC OPF [5]. However, many existing formulations rely on simplified network models or do not fully enforce static N-1 security under the nonlinear AC power flow model. Moreover, frequency constraints can lead to thin or fragmented feasible regions and cause solver difficulties, sometimes resulting in infeasibility [3].

Research that jointly enforces static N-1 security and explicit frequency security limits within an AC-SCOPF formulation remains limited. To the best of our knowledge, closely related representative studies include [6] and [7]. [6] embeds artificial neural network-based frequency indicators (trained from dynamic simulations) into an AC-SCOPF framework and demonstrates the method on a 39-bus system. In [7], a look-ahead dynamic security-constrained economic dispatch with frequency stability constraints is proposed, using linearized frequency dynamics and piecewise linearization AC power flow approximations. The method proposed in [7] was tested on an IEEE 118-bus system with a pre-selected contingency set rather than the full N-1 contingency list. These observations highlight the need for a scalable and robust FC-SC-ACOPF approach for larger networks and larger contingency sets.

This paper proposes a FC-SC-ACOPF model that simultaneously considers static N-1 security and frequency security while retaining the full AC power flow model. Scalability is enhanced by identifying dominant contingencies for optimization, while static security is verified against the full N-1 list and frequency security is validated via time domain simulations. In addition, we introduce the TJU method and a dynamic trajectory-based approach to improve solver robustness and identify potentially conflicting N-1 contingencies under frequency constraints. The framework is validated on a modified IEEE 14-bus system and the ACTIVSg 500-bus system.

It should be noted that this paper does not consider renewable energy uncertainty. Such deviations typically involve power fluctuations without a complete loss of generation, and the resulting active power imbalance is generally less severe than that of an N-1 generator outage. Consequently, frequency security constraints are more likely to be satisfied under the same reserve and inertia conditions. For the problem of renewable energy uncertainty, please refer to [8].

II. PROBLEM FORMULATION

In this section, we present the formulation of the FC-SC-ACOPF as follows:

$$\min f(\mathbf{x}_0,\mathbf{u}_0) \quad (1)$$

$$\text{s.t.} \quad \mathbf{g}_k(\mathbf{x}_k,\mathbf{u}_k)=0 \quad k\in\{0,1,2,...,N_{dc}\} \quad (2)$$

$$\mathbf{h}_k(\mathbf{x}_k,\mathbf{u}_k)\le 0 \quad k\in\{0,1,2,...,N_{dc}\} \quad (3)$$

979-8-3315-8138-1

where $k=0$ corresponds to the base case, N_{dc} is the total number of static dominant contingencies. Equation (1) defines the objective function, which minimizes the generation cost in the base case:

$$f(\mathbf{x}_0,\mathbf{u}_0)=\sum_{i=1}^{N_G} a_i P_{Gi,0}^2 + b_i P_{Gi,0} + c_i. \tag{4}$$

Equation (2) represents the equality constraints of the AC power flow equations in the base case and under the identified dominant contingencies, namely:

$$\begin{cases} P_{Gi,k} - P_{Li} - V_{i,k}\sum_{j\in i} V_{j,k}(G_{ij}\cos\theta_{ij,k} + B_{ij}\sin\theta_{ij,k}) = 0 \\ Q_{Gi,k} - Q_{Li} - V_{i,k}\sum_{j\in i} V_{j,k}(G_{ij}\sin\theta_{ij,k} + B_{ij}\cos\theta_{ij,k}) = 0 \end{cases} \quad i,j\in\{1,2,...,N_B\} \tag{5}$$

where $P_{Gi,k}$ and $Q_{Gi,k}$ are the active and reactive power output of generators at bus i in case k, respectively; $\theta_{i,k}$ is the voltage angle of bus i in case k and $\theta_{ij,k}=\theta_{i,k}-\theta_{j,k}$; $V_{i,k}$ are the voltage magnitude of bus i in case k; i,j denote the bus index and (i,j) represents the directed branch linking buses i and j; G_{ij} and B_{ij} are the conductance and susceptance of transmission line (i,j); N_B is the total number of buses.

Equation (3) represents the inequality constraints in the base case and the identified dominant contingencies, including:

1) *Operating constraints*

$$V_i^{\min} \le V_{i,k} \le V_i^{\max} \quad i\in\{1,2,...,N_B\} \tag{6}$$

$$\begin{cases} \left|S_{lf,k}\right| \le S_{lf}^{\max} \\ \left|S_{lt,k}\right| \le S_{lt}^{\max} \end{cases} \quad l\in\{1,2,...,N_L\} \tag{7}$$

$$\begin{cases} P_{Gi}^{\min} \le P_{Gi,k} \le P_{Gi}^{\max} \\ Q_{Gi}^{\min} \le Q_{Gi,k} \le Q_{Gi}^{\max} \end{cases} \quad i\in\{1,2,...,N_G\} \tag{8}$$

where $S_{lf,k}$ and $S_{lt,k}$ are the branch flow at the from bus and to bus of line l in case k, respectively; N_L denotes the total number of branches; N_G denotes the total number of generators; equation (6) represents the voltage magnitude limit, (7) represents the branch thermal limit, and (8) represents the real and reactive output limit of generators.

2) *Frequency response constraints*

We adopt the center of inertia (COI) concept and approximate the primary frequency response using a linear governor-ramp model [2]. Although these constraints represent post-contingency frequency response, their algebraic forms depend only on base case decision variables (generator active output $P_{Gi,0}$ and primary reserves R_{Gi}) and contingency-specific parameters (e.g., post-contingency inertia $M_{Hl,Sys}$). Therefore, they are included in $\mathbf{h}_0$ while being indexed by each generator outage l. The complete frequency security constraints are as follows:

$$\sum_{i\in N_G, i\ne l} R_{Gi} \ge P_{Gl,0}, \quad l\in\{1,2,...,N_{gl}\} \tag{9}$$

$$R_{Gi} \le \frac{2c_{gi}M_{Hl,Sys}(f_0 - f_{nadir})}{P_{Gl,0}}, \quad i\in\{1,2,...,N_G\}/\{l\}, l\in\{1,2,...,N_{gl}\} \tag{10}$$

$$R_{Gi} \le \overline{R_{Gi}}, \quad i\in\{1,2,...,N_G\}/\{l\}, \quad l\in\{1,2,...,N_{gl}\} \tag{11}$$

$$P_{Gi,0} + R_{Gi} \le P_{Gi}^{\max}, \quad i\in\{1,2,...,N_G\}/\{l\}, \quad l\in\{1,2,...,N_{gl}\} \tag{12}$$

$$\frac{P_{Gl,0}}{M_{Hl,Sys}} \le RoCoF_{\max}, l\in\{1,2,...,N_{gl}\} \tag{13}$$

where R_{Gi} is the primary reserve of generator i; c_{gi} is the maximum ramp rate of generator i; $M_{Hl,Sys}$ is the system inertia (MWs/Hz) after the loss of generator l; f_0 is the base frequency; f_{nadir} is the required frequency nadir; N_{gl} denotes the size of frequency dominant contingency set. Equation (9) represents the reserve adequacy constraint; (10) requires that the primary reserve should be delivered before the frequency reaches nadir; (11)-(12) represent the primary reserve bounds for capability and headroom, respectively; and (13) represents the RoCoF constraint. Due to the length limit, the detailed description of constraints (9)-(13) can be found in [2], [4].

3) *Coupling constraints*

$$P_{Gi,k} \ge P_{Gi,0} - P_{\max}^{rd} \quad k\in\{1,2,...,N_{dc}\} \tag{14}$$

$$P_{Gi,k} \le P_{Gi,0} + P_{\max}^{ru} \quad k\in\{1,2,...,N_{dc}\} \tag{15}$$

$$\begin{cases} (V_{i,k} - V_{i,0})(Q_{Gi,k} - Q_{Gi}^{\max}) \le 0 \quad k\in\{1,2,...,N_{dc}\} \\ (V_{i,k} - V_{i,0})(Q_{Gi,k} - Q_{Gi}^{\min}) \le 0 \quad k\in\{1,2,...,N_{dc}\} \end{cases} \tag{16}$$

where $P_{\max}^{rd}$ and $P_{\max}^{ru}$ are the maximum allowable ramp-down and ramp-up deviations from the base dispatch $P_{Gi,0}$, respectively. Equations (14)-(15) are introduced to couple the pre- and post-contingency state and equation (16) are used to approximate the post-contingency reactive response of generators.

Let $N_{DC,S}$ be the static dominant contingency set, N_{bc} be the total number of branch N-1 contingencies in $N_{DC,S}$, N_{gc} the total number of generator N-1 contingencies in $N_{DC,S}$. By adding slack variables $\hat{\mathbf{s}}^2$, the constraint set (5)-(16) can be arranged into a compact form as follows:

$$\begin{aligned} & H(\mathbf{x}) = \begin{bmatrix} C_E(\mathbf{x}) \\ C_I(\mathbf{x}) + \hat{\mathbf{s}}^2 \end{bmatrix} = \mathbf{0} : \Re^n \to \Re^m \\ & \mathbf{x} = (\mathbf{u}, \mathbf{y}, \hat{\mathbf{s}}^2(\mathbf{u},\mathbf{y})) \in \Re^n \\ & \mathbf{u} \in \Re^{3N_G - 1} \\ & \mathbf{y} \in \Re^{2N_B(N_{dc}+1)} \\ & \hat{\mathbf{s}}^2 = (s_1^2, ..., s_{4N_G+2N_B(N_{dc}+1)+2N_L+4N_{gl}+N_{bc}[2(N_L-1)+8N_G]+N_{gc}[2N_L+8(N_G-1)]}^2) \end{aligned} \tag{17}$$

where n and m are given by

$$n = 7N_G + 4N_B(N_{dc}+1) + 2N_L + 4N_{gl} + N_{bc}[2(N_L-1)+8N_G] + N_{gc}[2N_L + 8(N_G-1)] - 1,$$

$$m = 4N_G + 4N_B(N_{dc}+1) + 2N_L + 4N_{gl} + N_{bc}[2(N_L-1)+8N_G] + N_{gc}[2N_L + 8(N_G-1)].$$

By using (17), the feasible region of the FC-SC-ACOPF problem (1)-(3) can be expressed as:

$$FR_{FC} = \{\mathbf{u}\in\Re^{3N_G-1} : H(\mathbf{x}) = H(\mathbf{u},\mathbf{y},\hat{\mathbf{s}}^2(\mathbf{u},\mathbf{y})) = 0\}. \tag{18}$$

III. Solution Methodology

The computation burden of SCOPF grows significantly with system size and the number of considered contingencies [9]. In the FC-SC-ACOPF framework proposed by this paper, the introduction of frequency security constraints further tight-

979-8-3315-8138-1

ens the feasible region and increases the computational difficulty. This section presents a novel methodology to address these challenges.

A. Dominant Contingency Identification

Motivated by the observation that only a small subset of contingencies materially influences the optimal operating point, we employ a dominant contingency identification approach to identify a compact yet representative subset. The identification is performed separately for branch thermal violations, bus voltage violations, and post-contingency frequency response violations. This avoids conflating their different scales and ensures the comprehensive enforcement of both static and frequency security. Regarding frequency security, conventional OPF tends to fully dispatch the least-cost generators, which can lead to larger frequency deviations following the loss of such units. Accordingly, outages of generators with the top 10% active power output are considered as the initial set of dominant frequency contingencies.

Let N_C denote the set of candidate N-1 contingencies, N_{VT} the set of potential branch thermal violations, N_{VV} the set of potential bus voltage violations, $N_{DC,T}$ the dominant contingency set of branch thermal violations, $N_{DC,V}$ the dominant contingency set of bus voltage violations and $N_{DC,F}$ the dominant contingency set of frequency response violations. For violation $v \in \{N_{VV} \cup N_{VT}\}$ and contingency $k \in N_C$, let $\omega(v,k)$ be the violation magnitude of v under contingency k. Then a step-by-step description of the main process steps can be described as follows:

Step 1: Solve the base case OPF to obtain an operating point. Initialize the frequency-dominant contingency set $N_{DC,F}$ by selecting generator outages associated with the top-10% generators ranked by active power output.

Step 2: Solve the Frequency-Constrained ACOPF (FC-ACOPF) with respect to the frequency-dominant contingencies identified in step 1.

Step 3: Verify the solution by time domain simulation and, upon any violation, add the contingency causing new post-contingency frequency violation to $N_{DC,F}$. If no post-contingency frequency violation is found, go to the next step.

Step 4: Conduct static security assessment using AC power-flow calculations. Identify the static-dominant contingency set $N_{DC,S}$ using the following procedure. First, compute type-specific thresholds:

$$\begin{cases} \varpi_V = \alpha \max\limits_{v \in N_{VV}} \max\limits_{k \in N_C} \omega(v,k) \\ \varpi_T = \alpha \max\limits_{v \in N_{VT}} \max\limits_{k \in N_C} \omega(v,k) \end{cases} \quad (19)$$

where $\alpha \in (0,1)$ is a parameter controlling the size of the dominant contingency set. Then, for voltage violations, sort $v \in N_{VV}$ in descending order of $\max\limits_{k \in N_C} \omega(v,k)$. For each v, sort the contingencies $k \in N_C$ that cause v in descending order of $\omega(v,k)$. Select the first contingency that (i) is not already chosen and (ii) satisfies $\omega(v,k) > \varpi_V$ and add it to $N_{DC,V}$. If no contingency meets the condition, skip v. Apply the same procedure to thermal violations using ϖ_T, yielding $N_{DC,T}$. Finally, define the static-dominant set as $N_{DC,S} := N_{DC,T} \cup N_{DC,V}$.

Step 5: Solve the FC-SC-ACOPF with respect to both $N_{DC,F}$ and $N_{DC,S}$. Time domain simulation verification and static security assessment are carried out to check the solution. If no further violations are found, terminate the procedure and return the secure solution. Otherwise, go to step 2.

Note that in step 5, static security assessment is performed against the full N-1 contingency list and time domain simulation verification is performed for all single generator outages. In step 4, thresholds are introduced to control the problem size while preserving representativeness. Considering all violations is computationally burdensome and yields limited benefit. Although α is largely scale-robust due to its relative definition, the optimal setting can vary with grid scale; tuning may thus be needed for fundamentally different systems. In our numerical experience, choosing α between 0.3 and 0.5 provides a good trade-off between problem size and representativeness. We adopt 0.4 as a representative setting that consistently yields a compact yet reliable dominant contingency set in our test systems. Table I provides the comparison result for different settings of α on the 500-bus system.

Table I: Comparison Result for the Threshold Parameter

α	$N_{DC,S}$	Objective	Secure
0.2	223,224,229,156,402,311,175,8,9,287,157,356,54	81867.1848	True
0.3	223,224,229,156,402,311,175,8,9,287,157,356	81867.1796	True
0.4	223,224,229,156,402,311,175,8,9,287,157,356	81867.1796	True
0.5	223,224,229,156,402,311,175,8,9,287,157,356,64	81867.1848	True
0.6	223,224,229,156,402,311,175,8,9,287,157,356,64	81867.1848	True

B. TJU-Enhanced Interior Point Method

A standard interior point method may struggle to solve the FC-SC-ACOPF when security constraints markedly affect the feasible region. To improve calculation robustness, we adopt a two-stage strategy inspired by [10].

Stage 1: We first attempt to solve the FC-SC-ACOPF using a standard interior point method. If convergence is not achieved, a dynamical trajectory-based quotient gradient system (QGS) method [11] is employed to guide the initial search process towards the feasible region of problem (18). The QGS system corresponding to the FC-SC-ACOPF problem is constructed using (17):

$$\dot{x} = Q_H(x) = -DH(x)^T H(x) \quad (20)$$

where DH is the Jacobian matrix of $H(X)$. By *Theorem 6* in [11], QGS system (20) is completely stable. This property makes QGS an effective tool for assisting interior point method on difficult instances. However, full convergence can be time consuming for high-dimensional FC-SC-ACOPF. Therefore, we adopt a near-feasible point strategy that terminates the integration at a near-feasible point, thus preserving QGS's robustness while reducing runtime. In this paper, we start from a random initial guess and integrate the QGS system until the system mismatch $\|H(x)\|_\infty$ falls below 0.01. For a detailed description of QGS method, please refer to [11], [12].

Stage 2: the interior point solver is warm started with the near-feasible point from the first stage to compute the local optimal solution. This stage strictly enforces the full set of constraints defined in Section II and achieves full convergence.

It is observed that incorporating frequency security constraints may create potential conflicts with static N-1 security requirements, rendering several N-1 contingencies infeasible under frequency security limits, termed conflict contingencies. To address this, a dynamical trajectory-based approach is employed to identify such conflicts. According to QGS theory, each trajectory of the QGS system converges to an equilibrium manifold [11], [12]. Infeasibility leads the system to converge to a degenerate stable equilibrium point (DSEP), which captures mismatch information [11]. This property makes the QGS method an effective tool for assessing potential conflicts. Feasibility assessment is performed by constructing the corresponding QGS system (20) for the potential conflict contingencies and integrating it from 1000 random initial guesses. If all trajectories converge to DSEPs, the contingency is considered likely infeasible under the given frequency security constraints.

Table II provides a sensitivity analysis of the conflict contingency set with respect to f_{nadir}, illustrating how the strictness of the frequency security constraint affects the results.

Table II: Conflict Contingencies Under Different Frequency Nadir Limits

f_{nadir}	N-1 contingencies conflict with frequency security constraints
59.5 Hz	142,225,226,228,330,343,543
59.4 Hz	330,343,543
59.3 Hz	330,343,543
59.2 Hz	None

IV. Case Studies

This section presents numerical experiments on a modified IEEE 14-bus system and the ACTIVSg 500-bus system to evaluate the effectiveness of the proposed FC-SC-ACOPF formulation. Original case data are taken from [13-15]. The IPOPT solver [16] is used as standard interior point solver and ANDES [13] is used to validate the post-contingency frequency response via full time domain simulation. For the 14-bus system, configured as a low-inertia test case, the frequency nadir and RoCoF are set to 59.4 Hz and 0.8 Hz/s, respectively. For the 500-bus system, representing a large transmission grid with stronger primary frequency support, stricter limits of 59.5 Hz and 0.5 Hz/s are enforced.

A. Modified IEEE 14-bus System

In the 14-bus system, the original case is identified as likely infeasible for simultaneously enforcing both static and frequency security, as assessed with the QGS method. To ensure a feasible solution exists, the active power output limits of several generators and the thermal limits of several branches are slightly relaxed. Specifically, the active output limits of generators 2-5 are increased by 10 MW, and the thermal limits of branches 17-20 are raised by 10 MVA.

On the 14-bus system, considering all generators' and branches' N-1 contingencies yield 24 candidate contingencies (one removed for causing islanding). After applying the dominant-contingency identification method described in Section III-A, three contingencies are retained as dominant, significantly reducing the size of the contingency set. Based on the dominant contingencies obtained, we formulate the corresponding FC-SC-ACOPF problem.

In this case, the frequency and static security constraints substantially tighten the feasible region (see Figure 1), causing a flat-start IPOPT solve to terminate at an infeasible point. We therefore adopt the QGS-assisted strategy to restore solvability and a solution is obtained. Security assessment confirmed no further violations at this solution.

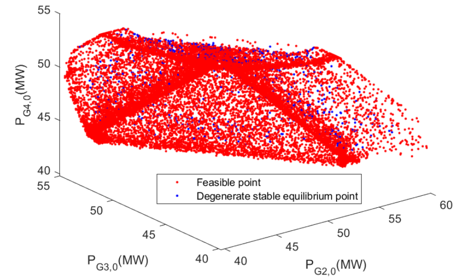

Figure 1. Feasible region of the 14-bus system under frequency security and static N-1 security constraints. The adjustment space for generator active output is very limited. The feasible region is characterized using the QGS method proposed in [11].

Table III and Figure 2 summarizes the comparison results between the AC OPF, FC-ACOPF and the proposed FC-SC-ACOPF.

Table III: Comparison Results for the 14-Bus System

Metrics	AC OPF	FC-ACOPF	FC-SC-ACOPF
Generation Cost	6730.93 $	7774.85 $	7790.40 $
Static viol.	17	2	0
Freq. viol.	1	0	0
Worst Nadir	58.4023 Hz	59.4013 Hz	59.4357 Hz
Worst RoCoF	2.0408 Hz/s	0.7900 Hz/s	0.7670 Hz/s

Static/Freq. viol.: number of contingencies with static/frequency violations.

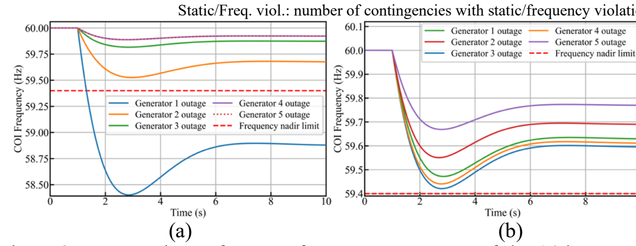

Figure 2. Comparison of system frequency responses of the 14-bus system obtained using two methods under N-1 contingencies of the top three largest generation units. (a) AC OPF. (b) FC-SC-ACOPF.

B. ACTIVSg 500-bus System

For the 500-bus system, the initial contingency set contains 681 N-1 contingencies, of which 220 branch contingencies cause islanding. With the assistance of QGS method, 7 branch contingencies are identified as very likely infeasible under the frequency security constraints. After preprocessing, a set of 454 contingencies remains for subsequent steps. We formulate and solve the FC-SC-ACOPF in an iterative way. In this case, 56 generators are online, and 6 corresponding contingencies are identified as frequency dominant. For conciseness, only the time domain simulation results are presented for outages of these generators. Though not presented, none of other generators' outage causes post-contingency frequency response violation. The static dominant contingency identification results are reported in Table IV.

The security assessment after the 2nd iteration shows no further violation. Detailed results are reported in Table V and Figure 3. Table V shows the trade-off: FC-SC-ACOPF eliminates static and frequency violations at a 12.8% cost increase compared to the AC OPF.

Table IV: Static Dominant Contingency List

Iteration	Violation Index	Ranked Contingencies[a]	Dominant Contingency
1	Bus 181	156, 402, 157	156
	Bus 182	156, 402, 157	402
	Bus 208	311	311
	Bus 110	175,8,9,287,174,607	175
	Bus 316	8,9,287,174	8
	Bus 317	8,9,287,174	9
	Bus 111	175,8,9,287,174,607	287
	Bus 487	156, 402, 157	157
	Bus 242	356	356
	Branch 227	224	224
	Branch 228	223	223
2	Branch 144	229	229

a. Contingencies causing corresponding violation ranked in descending order by violation magnitude.

Table V: Comparison Results for the 500-Bus System

Metrics	AC OPF	FC-ACOPF	FC-SC-ACOPF
Generation Cost	72578.30 $	79012.35 $	81860.54 $
Static viol.	244	242	0
Freq. viol.	3	0	0
Worst Nadir	59.1666 Hz	59.5031 Hz	59.5028 Hz
Worst RoCoF	0.9370 Hz/s	0.4342 Hz/s	0.4665 Hz/s

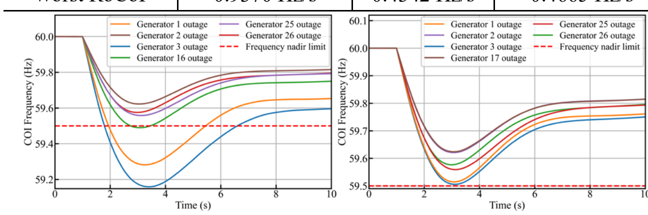

(a) (b)

Figure 3. Comparison of system frequency responses of the 500-bus system obtained using two methods under N-1 contingencies of the top three largest generation units. (a) AC OPF. (b) FC-SC-ACOPF.

C. Computational Time Breakdown

We report a time breakdown of the proposed methodology in Table VI. The TJU stage is activated only when IPOPT fails to converge. Since IPOPT converges directly in the ACTIVSg 500 case, the corresponding TJU stage time is reported as "–" (not invoked).

Table VI: Computational Time Breakdowns for the Test Cases

System	Dom. Cont. Identification	TJU stage	IPOPT solve
Modified IEEE-14	0.4075s	2.663s	0.319s
ACTIVSg-500	14.2670s	-	75.0832s

Dom. Cont.: Dominant Contingency.

V. Conclusion

This paper proposes a solution methodology that jointly enforces static N-1 security and frequency response constraints. The main contributions are: (1) the integrated SC-AC power flow model with frequency response constraints, (2) a dominant contingency identification method to enhance the scalability for large contingency sets, and (3) the implementation of trajectory-based method to improve calculation robustness and identify potential conflicts between static N-1 security and frequency security. Case studies on the 14-bus system and the 500-bus system serve to validate the effectiveness of the proposed methodology. Future work will consider introducing more precise nonlinear frequency constraints while maintaining computational tractability and developing efficient solution methodologies for larger scale FC-SC-ACOPF.

References

[1] N. Nguyen, S. Almasabi, A. Bera, and J. Mitra, "Optimal power flow incorporating frequency security constraint," *IEEE Trans. Ind. Appl.*, vol. 55, no. 6, pp. 6508–6516, 2019.

[2] H. Chávez, R. Baldick, and S. Sharma, "Governor rate-constrained OPF for primary frequency control adequacy," *IEEE Trans. Power Syst.*, vol. 29, no. 3, pp. 1473–1480, 2014.

[3] W. Xu, Z. Chu, F. Capitanescu, and F. Teng, "On the incorporation of stability constraints into sequential operational scheduling," in *Proc. 2025 IEEE Power & Energy Society General Meeting (PESGM)*, Jul. 2025, pp. 1–5.

[4] R. Zhang, Y. Chen, K. Yan, Z. Li, T. Jiang, G. Li, and X. Li, "Incorporating frequency security constraints in two-stage robust unit commitment of integrated transmission and distribution system," *IEEE Trans. Sustain. Energy*, vol. 17, no. 1, pp. 70–86, 2026.

[5] X. Zhao, H. Wei, J. Qi, P. Li, and X. Bai, "Frequency stability constrained optimal power flow incorporating differential algebraic equations of governor dynamics," *IEEE Trans. Power Syst.*, vol. 36, no. 3, pp. 1666–1676, 2020.

[6] M. I. Alizadeh, F. Capitanescu, P. P. Barbeiro, J. Gouveia, C. L. Moreira, and F. Soares, "Extending AC security-constrained optimal power flow for low-inertia systems with artificial neural network-based frequency stability constraints," in *Proc. 2024 IEEE PES Innovative Smart Grid Technologies Europe (ISGT Europe)*, Oct. 2024, pp. 1–5.

[7] M. Javadi, T. Amraee, and F. Capitanescu, "Look-ahead dynamic security-constrained economic dispatch considering frequency stability and smart loads," *Int. J. Electr. Power Energy Syst.*, vol. 108, pp. 240–251, 2019.

[8] L. Zeng and H. D. Chiang, "Online and Look-Ahead Determination of the Renewable Admissible Region for Managing the Uncertainty of Renewables: Theory and Some Applications," *IEEE Trans. Power Syst.*, vol. 39, no. 4, pp. 5609-5619, July 2024.

[9] F. Capitanescu, J. M. Ramos, P. Panciatici, D. Kirschen, A. M. Marcolini, L. Platbrood, and L. Wehenkel, "State-of-the-art, challenges, and future trends in security constrained optimal power flow," *Electr. Power Syst. Res.*, vol. 81, no. 8, pp. 1731–1741, 2011.

[10] T. Li, H. D. Chiang, and Z. Y. Wang, "A novel trajectory-unified method for AC optimal power flow," in *Proc. 2024 IEEE Power & Energy Society General Meeting (PESGM)*, Jul. 2024, pp. 1–5.

[11] H. Chiang and C. Jiang, "Feasible region of optimal power flow: Characterization and applications," *IEEE Trans. Power Syst.*, vol. 33, no. 1, pp. 236–244, Jan. 2018.

[12] H. D. Chiang and Luís F. C. Alberto, *Stability Regions of Nonlinear Dynamical Systems: Theory, Estimation, and Applications*, Cambridge University Press, Cambridge, 2015.

[13] H. Cui, F. Li, and K. Tomsovic, "Hybrid symbolic-numeric framework for power system modeling and analysis," *IEEE Trans. Power Syst.*, vol. 36, no. 2, pp. 1373–1384, 2020.

[14] A. B. Birchfield, T. Xu, K. M. Gegner, K. S. Shetye, and T. J. Overbye, "Grid structural characteristics as validation criteria for synthetic networks," *IEEE Trans. Power Syst.*, vol. 32, no. 4, pp. 3258–3265, Jul. 2017.

[15] T. Xu, A. B. Birchfield, and T. J. Overbye, "Modeling, tuning, and validating system dynamics in synthetic electric grids," *IEEE Trans. Power Syst.*, vol. 33, no. 6, pp. 6501–6509, 2018.

[16] A. Wächter and L. T. Biegler, "On the implementation of an interior-point filter line-search algorithm for large-scale nonlinear programming," *Math. Program.*, vol. 106, no. 1, pp. 25–57, 2006.

979-8-3315-8138-1